Interreg

Co-funded by the European Union

Italy – Croatia

STRENGTH

D.1.3.2
Geophysical measures in river embankments

Interreg Co-funded by the European Union

Italy – Croatia

STRENGTH

Project acronym	STRENGTH
Project full title	STRategies for assessing climate change and natural hazards' impact on urban ecosystems, increasing resilience to ENvironmental hazards, and promoting territorial GrowTH
Programme	Interreg Italy-Croatia 2021-2027
Start date	01/04/2024
End date	30/09/2026
Project ID	ITHR0200318

Deliverable Title	D.1.3.2 - Geophysical measures in river embankments
Activity	1.3 -Geophysical measures campaign for seismic and hydraulic vulnerability
WP	WP1 - Monitoring, measuring, and early warning systems
WP Leading Partner	CORA
Contributing Partners	OGS, CBPF
Dissemination level	Confidential
Version	Finalised
Date	28/05/2026

Table of contents

1. Introduction

The study of embankments is crucial due to their role in flood control, particularly in the context of climate change and the increasing frequency of extreme weather events. Embankments are vital structures that protect urban, agricultural, and environmental areas from flooding, and understanding their condition is key to maintaining their effectiveness.

In Italy, and particularly in the Comacchio area (province of Ferrara, northern Italy), the region is highly susceptible to flood events due to its geographic and hydrogeological characteristics, including the presence of wetlands and the low-lying deltaic landscape. This makes the region vulnerable to flash flooding, exacerbated by climate-related changes (de Oliveira and Bonetti, 2021; Bonetti et al., 2022).

The study area lies in the eastern sector of the Po River plain, within the Comacchio region - an area of reclaimed land characterized by flat topography. The subsurface geology consists of a thick accumulation of Quaternary sediments, reaching depths of 700–800 m in the Po Basin. These deposits reflect a long-term evolution driven by sea-level fluctuations, beginning with alluvial plain sediments laid down during the regressive phase leading to the Last Glacial Maximum, and subsequently overlain by retrogradational coastal and estuarine facies, followed by progradational deltaic deposits. The resulting stratigraphy is complex and includes alternating layers of fine-grained silts and clays, as well as coarser sands and gravels, often linked to paleo-channel systems (Castellarin et al., 1985; Amorosi et al., 2003).

In flood-prone areas such as the Comacchio region, it is important to assess the structural integrity and overall condition of embankments. The main issues for embankments include structural weaknesses related to erosion, material deterioration, seepage, and piping, as well as variability in subsurface conditions. The heterogeneity of the material is therefore an important factor to consider when analyzing embankment stability. The analysis of the embankment's geology is also crucial to assess potential phenomena such as increased pore water pressure (which may result from heavy rainfall or flooding), leading to reduced shear strength resistance. The mechanisms of embankment failure are closely related to changes in the hydraulic regime of river flow. Prolonged high-water levels can weaken the structure by reducing its resistance, while a rapid drop in water level (e.g., during the recession phase of an overflow event) can induce seepage forces directed toward the streamside, potentially leading to internal erosion.

The aim of this study is to analyze a section of the embankment near Ponte Lanzoni, along the "Canale Circondariale Gramigne Fosse" in the Comacchio area, and to apply geophysical methods to identify and characterize potential weak zones within the embankment structure. This specific study area was selected due to its frequent impact during flood events and its susceptibility to flood-related damage and the formation of "fontanazzi" (Bernatek-Jakiel and Poesen, 2018).

The summer 2024 geophysical exploration campaign in Ponte Lanzoni is part of an effort to increase resilience to flash flooding and reduce possible urban, agricultural, and environmental damages. Geophysics, and particularly the integration of different geophysical methods (active seismic, geoelectrical acquisition, Ground Penetrating Radar (GPR), and others), allows for a comprehensive assessment of embankment health. These techniques are useful for analyzing potential weaknesses in the embankments, providing crucial information for future strengthening and modification efforts. In cases where extreme events may occur before embankment reinforcement, these data can help predict potential damage.

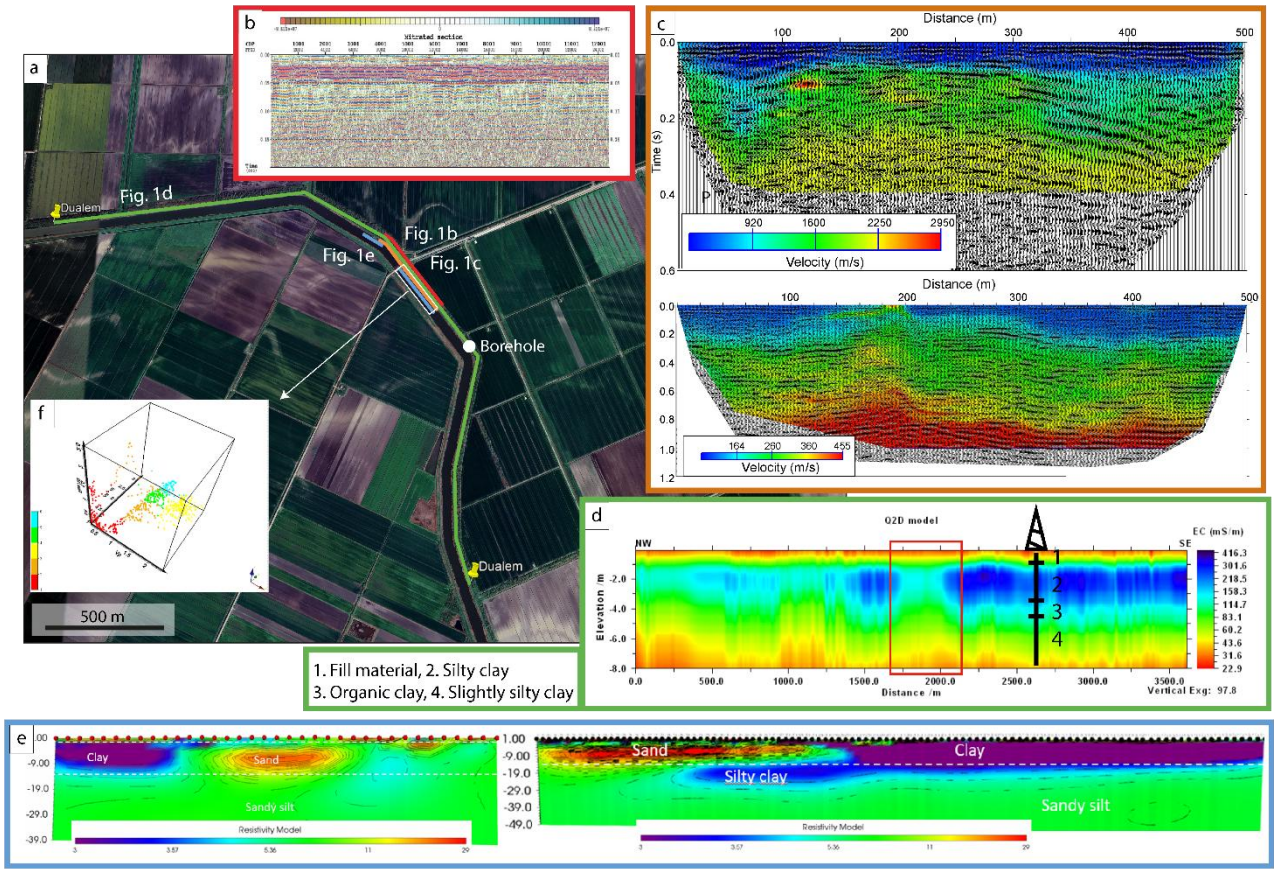

Figure 1 *Position of the different surveys and resulting profiles.* ***a.*** *Map of the study area (from Google Earth) and survey location. Red line: GPR data; orange line: P and S seismic data; blue line: ERT data; green line: Dualem data.* ***b.*** *GPR profile* ***c.*** *Seismic reflection time section (P waves above, S waves below) overlying the tomographic velocity model.* ***d.*** *Results of the Dualem data inversion with borehole stratigraphy.* ***e.*** *Electric resistivity tomographic models ERT2 (left) and ERT1 (right).* ***f.*** *3D display of the clustering analysis computed on P and S waves velocities and resistivity.*

2. Data and methods

Different geophysical methods were used in this study (location in Fig. 1), including seismic surveys with P and S waves, Electrical Resistivity Tomography (ERT), Ground Penetrating Radar (GPR) acquisition and Electromagnetic induction (EMI). The data were processed,

analyzed, and interpreted. Subsequently, all datasets were integrated both at the interpretation level and for clustering purposes.

2.1 Seismic data

Seismic reflection data and P- and S-wave tomography give information not only about the subsoil geometries and velocity distribution, but, especially if integrated with other methods, it allows the estimation of stiffness, degree of consolidation, material type, and pore saturation, as well as to detect weak or unconsolidated zones potentially affected by internal erosion (e.g., piping) (Deidda and Ranieri, 2005; Fauchard and Mériaux, 2007; Accaino et al., 2023). P-wave tomography is particularly sensitive to material density, bulk modulus, and pore saturation (i.e., groundwater level), while S-wave tomography is mostly sensitive to shear modulus (i.e., mechanical strength) and soil consolidation state. By combining both P- and S-wave tomographic results, it is possible to compute advanced geotechnical parameters such as the Vp/Vs ratio, which may provide further insights into lithological contrasts, pore fluid content, and mechanical behavior. These integrated datasets can be used to infer shear strength and assess the stability conditions of the embankment.

Seismic Data Acquisition

Three NW–SE-oriented seismic profiles were acquired in the study area. The seismic source used was the Electrodynamic Vibrator System ELVIS VII (Geosym), a portable transverse vibrator capable of delivering a maximum force of 1 kiloNewton. This source is particularly well-suited for very shallow seismic investigations targeting depths of less than 200 meters. Thanks to its relatively low weight and its mounting on a detachable wheelbarrow frame, the ELVIS VII is highly portable and adaptable to various field conditions. The system can generate either SH or SV waves depending on the sweep direction, and it supports frequency sweeps ranging from 10 to 320 Hz, with sweep durations of 10 to 12 seconds. Shot points and receivers were spaced every 2 meters and every 4 meters, respectively. Data acquisition was performed using a 16-second sweep length, a 1 ms sampling rate, and a frequency range of 20 to 180 Hz. One sweep was recorded for the P-wave profile and two sweeps for the S-wave profile.

South of the Lanzoni Bridge, a 300-meter-long segment (150 active channels) was acquired using both NuSeis 3-component (3C) nodes and single-component geophones (14 Hz LGT-20D4.5 horizontal geophones for S waves and SM10 vertical geophones for P waves). This dual setup allowed for a direct image of the seismic data, which is not obtainable using only

3C geophones. The full 500-meter seismic profile (orange line in Fig. 1) was acquired using 250 channels with NuSeis Node NRU N3 systems, manufactured by Geophysical Technology, Inc. These are three-component seismic recorders equipped with three internal orthogonal geophones, enabling the acquisition of full-wavefield 3C seismic data. The sweep length was 16 seconds, with a 1 ms sampling rate and a frequency range of 30 to 240 Hz.

Data were collected using the telemetric X One DMT Summit seismic acquisition system, which is based on channel boxes (A/D converters) connected via a lightweight two-wire cable. This cable powers the sensors and transmits the acquired signal. Each module was connected to a Data Collector powered by a car battery.

To ensure accurate geometric positioning of both receivers and source points for subsequent data processing—such as topographic corrections in travel-time tomography and proper migration of reflected signals—a detailed topographic survey was conducted. All surveying operations employed real-time differential GNSS positioning techniques using the VRS (Virtual Reference Station) method.

Seismic data processing

To facilitate the picking of first arrivals for tomographic inversion, we applied deconvolution prior to the cross-correlation of the data with pilot traces (Baradello and Accaino, 2016). Shots acquired at the same locations were stacked to enhance the signal-to-noise ratio. Subsequently, we applied filtering techniques to suppress both random and coherent noise, followed by automatic gain control (AGC) to amplify signal amplitudes, particularly at larger offsets.

A different processing workflow was implemented to enhance reflection seismic imaging and suppress both coherent and random noise. For the pre-stack P-wave data, we applied zero-phase deconvolution and trimmed mean-dynamic dip filtering (TMDDF) to partially attenuate ground roll. Stacking velocity analysis was performed on pre-stack data sorted into common depth point (CDP) gathers, and the resulting velocity model was used to apply normal moveout (NMO) correction, followed by stacking of the CDP gathers. After time migration, FX deconvolution was applied to the migrated data to improve the horizontal continuity of the reflected signals.

For the SH-wave data, the same processing steps were applied, except for zero-phase deconvolution, which did not yield satisfactory results in this case.

Seismic tomography

We performed first-break seismic tomography using the CAT3D software developed by OGS (Böhm et al., 2014), which is based on minimum-time ray tracing (Böhm et al., 1999). The process began with manual picking of first arrivals on common-shot gathers for both P- and S-waves, typically excluding near-offset traces to avoid contamination from ground roll.

Travel-time inversion was then applied to derive the P- and S-wave velocity structure of the subsurface. CAT3D employs the simultaneous iterative reconstruction technique (SIRT) for tomographic inversion. To improve resolution while maintaining stability, we implemented the staggered grid approach (Vesnaver and Böhm, 2000). This method begins with a coarse starting grid, minimizing the null-space and ensuring a well-posed problem. The grid is then shifted multiple times in both X and Y directions, generating several offset grids. An independent inversion is performed for each, and the results are subsequently averaged to produce a refined final velocity model that retains the advantages of the original coarse-grid inversion.

Variations in seismic velocity are interpreted as changes in subsurface properties such as lithology, stiffness, and fracturing. Finally, the depth-interval velocity sections derived from first-break tomography were superimposed on the seismic sections to verify the consistency between the positions of reflecting horizons and the derived velocity fields.

2.2 The Electrical Resistivity Tomography (ERT)

Electrical Resistivity Tomography (ERT) widely applied in embankment stability studies (e.g., Niederleithinger et al., 2012; Araújo et al., 2023), was employed to investigate the subsurface resistivity distribution, which is sensitive to fluid content, porosity, and degree of saturation. The two acquired profiles are both located on the crest of the embankment (blue lines in Fig. 1).

Data acquisition

We employed a Multi-Source Wireless Data Acquisition System (MPT3D, Multi-Phase Technology) that includes 12 stand-alone transceivers, each synchronized via GPS timing and controlled through a 900 MHz wireless radio protocol. Each unit manages up to three electrodes. A dipole–dipole array configuration and a 1000 mA current were used for both ERT1 and ERT2. Measured resistance values ranged from 10 to 300 Ω·m for all adjacent

electrode pairs, indicating good acquisition conditions. For the ERT 1 profile we used 108 electrodes spaced 4 m, for total survey length of 321 m, while for the ERT 2 profile the electrode spacing was 3 m, for total survey length of 140 m. The maximum effective investigation depth for ERT1 and ERT2 is approximately 50 and 20 m, respectively.

Data Processing

Main objective of the data processing is to obtain the apparent resistivity values, calculated from the measured potential differences (V) and current intensities (I). The data were then inverted to generate true resistivity models of the subsurface.

The data were processed using a standard 3D geophysical inversion workflow. Individual acquisitions were first aggregated, and the topographic data (referenced to UTM32 – WGS84) were imported. A 3D mesh was then generated, with cells defined along the x, y, and z axes. To minimize the extent of the background region, the mesh was rotated and translated accordingly. Based on the median apparent resistivity values, we selected a slightly higher value—6.5 Ωm—as the starting model for the inversion. A noise level of 2–3% was applied to the resistivity data. The inversion was performed with a recalculation of the roughness parameter at each iteration, allowing up to four iterations for a full inversion.

Data processing was carried out using ERTLab Studio software, which performs inversion using the least squares method with regularization. This approach, commonly referred to as "Occam's inversion" in literature, minimizes the residuals between the calculated and observed pseudosections to obtain a geologically plausible resistivity distribution.

2.3 GPR data

GPR surveys use an antenna that emits electromagnetic waves and then receives the echo generated by buried targets (Davis and Annan, 1989). The penetration of the electromagnetic waves depends on the conductivity of the earth material, with dry materials such as sand and rock having good penetration (Smith and Jol, 1995). Water content significantly affects GPR wave velocity, as it increases the dielectric constant ε. Since water has an ε around 80—much higher than that of dry soils—it causes noticeable velocity variations ($V = c/\sqrt{\varepsilon}$).

The use of Ground Penetrating Radar (GPR) can support the detection of shallow features such as animal burrows, voids, and structural discontinuities within river embankments (Di Prinzio et al., 2010), providing high-resolution insights into near-surface conditions, very

important for embankment characterization (e.g., Szynkiewicz, 2000; Mori, 2009; Perri et al., 2014). When combined with other geophysical methods—as in our study—GPR data enhances the characterization of near-surface conditions. It is particularly effective in identifying shallow features such as stratigraphic discontinuities, buried utilities, and remnants of previous constructions within or beneath levee systems, providing high-resolution insights into the subsurface structure. We collected 2 profiles of 500 m length (round trip) on the top of the embankment in correspondence of the 3C seismic profile (orange line in Fig. 1).

Data acquisition

The GPR method was used here to investigate the first few meters of soil within the embankments. A GSSI SIR-4000 ground-penetrating radar equipped with a monostatic antenna—i.e., a single dipole functioning as both transmitter and receiver (zero-offset configuration)—was employed. Frequencies of 100 and 200 MHz were selected based on the expected clay-rich soil conditions (Baradello and Accaino, 2016). A time window of 500 and 300 ns was used for respectively the 100 MHz and 200 MHz antennas.

We carried out the GPR profiles using the distance data acquisition method with a survey wheel. A person drives the radar along the line at a constant speed, and the antenna transmits the signals into the ground and records the data at an arbitrary distance of 2 cm 8 (i.e. 50 ScanPerMeters).

Data processing

GPR data were converted to SEGY format and processed in Paradigm FOCUS 5.4 to enhance reflected signals and reduce noise. Geometry was assigned to each trace, with X-coordinates starting from zero at the seismic profile's origin. A Butterworth bandpass filter (60–240 MHz for the 100 MHz profile, based on spectral analysis) was applied to suppress high-frequency noise and direct currents components. A 2D spatial filter was used to mitigate ringing effects. For each profile, an average amplitude decay curve was computed, and its inverse applied as a gain function to preserve anomaly intensity contrasts. Finally, an f-K migration was applied using an EM wave velocity of 7 cm/ns, consistent with clay-rich ground conditions, to improve the resolution of subsurface features.

2.4 Electromagnetic Induction in the frequency domain

The method is based on the principle of electromagnetic induction and allows rapid, non-invasive mapping of spatial variations in the electrical conductivity of subsurface materials. It is often used as a complement to other geophysical methods (Fauchard and Mériaux, 2007, Inazaki, 2007; Cygal et al., 2016).

Data acquisition

Around 3.5 km of line were acquired with the DUALEM-642S system. This consists of a transmitting coil and two receiving coils arranged in dual-coil configurations—Horizontal Co-Planar (HCP) and Perpendicular (PRP)—with coil separations at 2, 4, and 6 meters. This configuration allows for multiple depth readings, providing six simultaneous levels of electrical conductivity measurements. The system operates at a frequency of 9 kHz and has a theoretical maximum investigation depth of approximately 9 meters. The EMI survey covered approximately 3,500 linear meters of profile length (white line in Fig. 1), with measurements taken at an average spacing of 1.4 meters.

Data processing

Electromagnetic (EM) data can be inverted to calculate true electrical conductivity (σ–mS/m) (Huang et al., 2016 and references therein). Data processing was carried out using the EM4Soil software package, which performs electromagnetic data inversion using a 2D smoothness-constrained approach. EM4Soil allows for both direct electromagnetic modeling and the inversion of induction data, facilitating the construction of conductivity models of the subsurface.

3. Results and interpretation of the geophysical data

3.1 Seismic data

The acquired seismic profiles image subsurface geometries down to ~0.6 s TWT for P-waves and ~1.1 s TWT for S-waves. Tomography results show a general velocity increase with depth, with significant lateral heterogeneities. Overlaying the data (Fig. 1c), we can appreciate a

strong correspondence between velocity variations and seismic facies changes, indicating lithological contrasts. A near-surface low-velocity layer (<1 km/s) extends to ~10–15 meters depth, with notable lateral variability. Deeper intervals show higher velocities and stronger reflectors. Between the beginning of the profile and 150 m, and then again between 320 and 400 m, lower seismic velocities and discontinuous seismic horizons suggest the presence of channel-like features up to a calculated depth of around 15 m. At 200 and 300 m along the profile, the signal is influenced by the presence of the roads.

3.2 Electric resistivity data

The inversion of the electrical resistivity data from profile ERT1 (Fig. 2) reveals three main horizontal layers. The uppermost layer, extending to about 2 meters depth, corresponds to the embankment and shows low resistivity. Below this, the second layer represents the natural soil north of the embankment, extending down to about 14 meters. This layer exhibits significant lateral heterogeneity, with a thin layer of intermediate resistivity followed by a high-resistivity lens (red in Fig. 2), likely representing a paleo-channel. Between electrodes 39 and the end of the profile, low resistivity values (violet in Fig. 2) suggest clay-rich deposits. The deepest layer, with intermediate resistivity (green in Fig. 2), is interpreted as a coarser sedimentary sequence.

model ERT1.

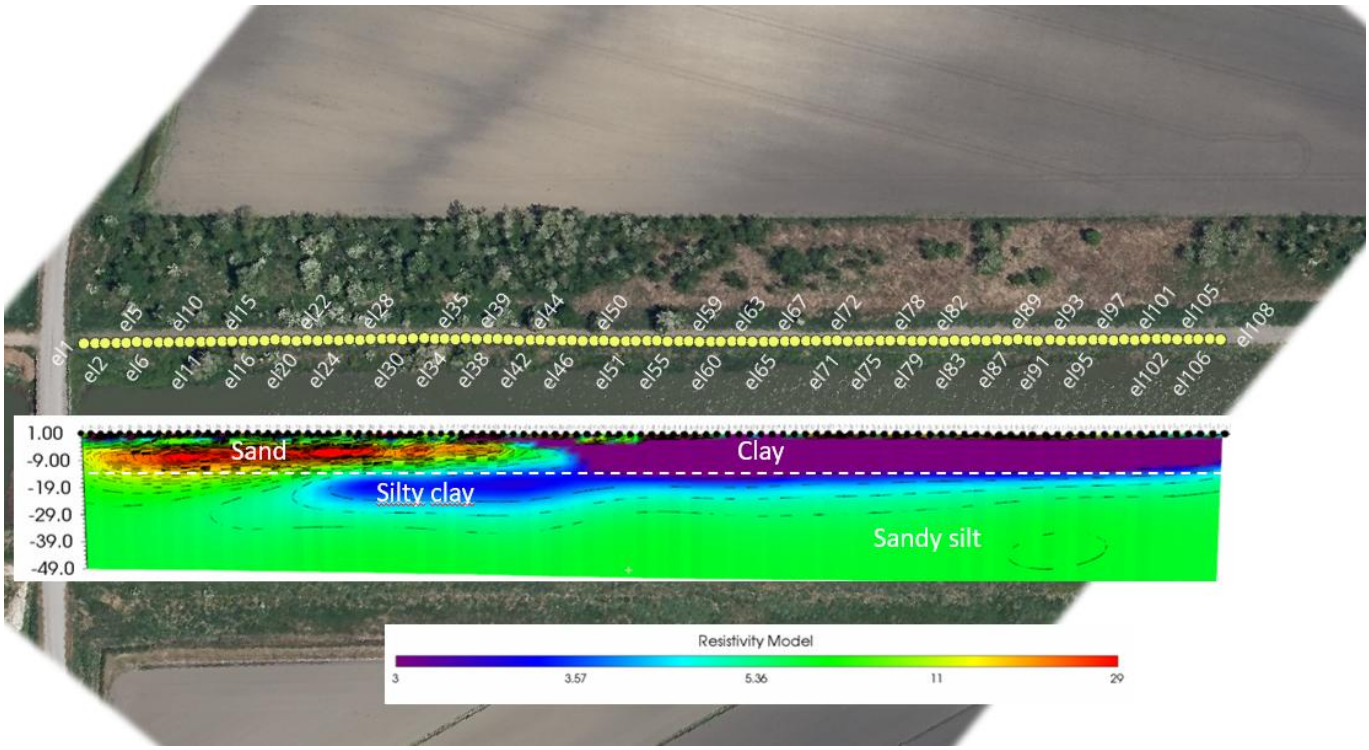

Fig. 2: Resistivity model derived from ERT1.

In the resistivity model derived from ERT2 (Fig. 3), the embankment shows similar sedimentary characteristics with significant variations in grain size, alternating between coarser and finer zones. Coarse materials, associated with paleo-channels, exhibit high resistivity (orange to red in Fig. 3), while finer deposits correspond to areas that were not affected by watercourses (blue to violet in Fig. 3).

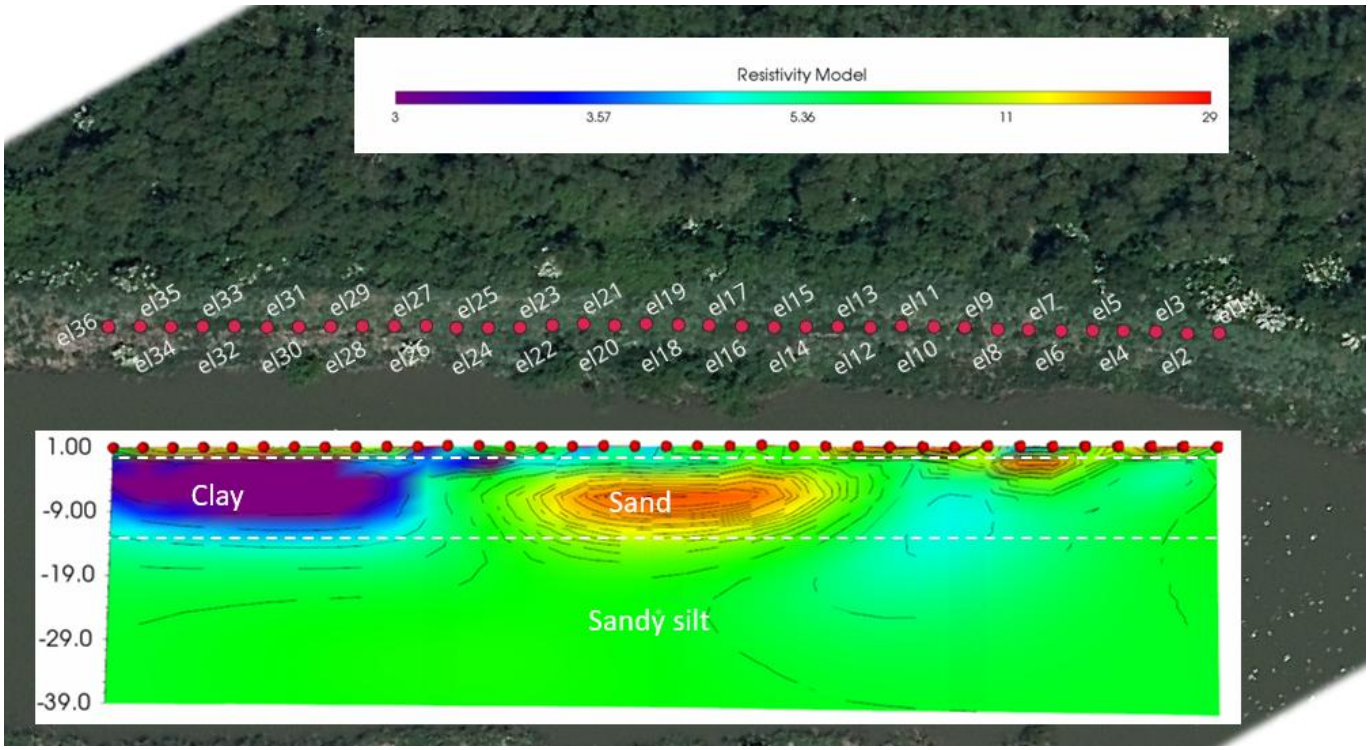

Fig. 3: Resistivity model derived from ERT2.

3.3 GPR data

GPR results complement seismic and ERT data by providing high-resolution insights into near-surface conditions and construction-related features (Perri et al., 2014). The analysis of the GPR profiles recorded on the top of the embankment clearly shows the presence of some very shallow reflectors characterized by several discontinuities and phase changes. These features can be associated with different compositions of clay materials.

3.4 Electromagnetic (Dualem) data

The electrical conductivity model derived from the DualEM data (Fig. 1d) reveals a shallow surface layer (~1 m thick) with conductivity values around 22 mS/m. Beneath this, a highly conductive layer extends from 2 to 4 m depth, with values ranging from 120 to 420 mS/m. A deeper layer shows intermediate conductivity values between 22 and 83 mS/m. The first half

of the profile generally exhibits lower conductivity, while the second half shows a more pronounced and continuous conductive layer. The conductive zone is likely associated with finer-grained materials like silts and clays, whereas the more resistive zone at greater depths likely corresponds to coarser sediments with a lower loamy-clayey fraction. The profile intersects a borehole, allowing for calibration and lateral extrapolation of point-scale data.

4. Discussion

As highlighted in previous studies (e.g., Inazaki, 2007; Perri et al., 2014), geophysics is a key tool for assessing the health of flood-control embankments. Visual inspections and point measurements alone may not be sufficient to detect subsurface anomalies such as internal erosion, voids, or preferential flow paths caused by variations in grain size or animal activity. Geophysical techniques allow for the identification of these critical features, providing engineers with actionable information to target areas that may require reinforcement, monitoring, or remediation.

The integrated geophysical approach effectively identified key subsurface features, such as paleo-channels, which have been identified through several geophysical datasets. Coarse-grained bodies were clearly detected in the electrical resistivity profiles, and their spatial distribution corresponds well with features observed in the orthophotos, supporting their interpretation as relict fluvial channels. These structures pose a risk to embankment stability, as the coarser nature of their lithology makes them highly permeable and could facilitate rapid water infiltration, leading to potential instability, internal erosion or piping during floods. In contrast, clay-rich zones provide better hydraulic sealing but can experience reduced shear strength when saturated, increasing the likelihood of localized instability or failure (Fauchard and Mériaux, 2007; Perri et al., 2014). Stratigraphic data confirm the interpretation, with alternating layers of fine and coarse sediments, influenced by the local hydrogeological setting.

5. Conclusions

Understanding the geological materials' spatial distribution is crucial for risk assessment and targeted interventions, ensuring the embankment's long-term resilience (Inazaki, 2007; Perri et al., 2014). This study demonstrates the effectiveness of integrating multiple geophysical methods to assess embankment stability. The identification of paleo-channels filled with gravel and clay-rich zones emphasizes the need for detailed subsurface mapping. Gravel-

rich areas pose risks of water infiltration and internal erosion, while clayey areas, though providing sealing, can lose strength when saturated.

6. Next steps

Considering that a portion of the study area was investigated using multiple geophysical methods, we are working on a 3D multi-parameter clustering approach based on P- and S-waves velocities and electrical resistivity models. This method aims to subdivide the subsurface into zones with internally consistent geophysical properties (Accaino et al., 2023). Preliminary clustering results, obtained using the k-means algorithm (Benjumea et al., 2023), are shown in Fig. 1f. We will use these clusters to perform a petrophysical inversion of the clusters, to infer the clay content, porosity and water saturation, as described by Accaino et al. (2023).

7. References

Accaino, F., Da Col, F., Böhm, G., Picotti, S., Giorgi, M., Meneghini, F., Schleifer, A., 2023. Petrophysical characterization of the shallow sediments in a coastal area in NE Italy from the integration of active seismic and resistivity data. Surveys in Geophysics, 44 (4), 1211-1238. https://doi.org/10.1007/s10712-023-09776-x

Amorosi A, Centineo M C, Colalongo M L, Pasini G., Sarti G, Vaiani S C, 2003. Facies architecture and Latest Pleistocene-Holocene depositional hystory of the Po Delta (Comacchio area), Italy. The Journal of Geology, vol. 111, p. 39-56, ISSN: 0022-1376.

Araújo, O. S., Picotti, S., Francese, R. G., Bocchia, F., Monteiro Santos, F., Giorgi, M., and Tessarollo, A., 2023. Frequency domain electromagnetic calibration for improved detection of sand intrusions in river embankments. The Leading Edge, 42, 615–624. doi: 10.1190/tle42090306.1.

Baradello L., Accaino F., 2016. GPR and high resolution seismic integrated methods to understand the liquefaction phenomena in the Mirabello Village (earthquake ML 5.9, 2012). Eng Geol 211:1–6. https://doi.org/10.1016/j.enggeo.2016.06.027

Benjumea, B., Gabàs, A., Macau, A., Bellmunt, F., Ledo, J., Ripoll, J., Figueras, S., 2023. Geomechanical parameters assessment and geological characterization using fuzzy C means clustering of electrical resistivity and seismic data. Near Surface Geophysics 21, 429–443. https://doi.org/10.1002/nsg.12247

Bernatek-Jakiel, A., Poesen, J., 2018. Subsurface erosion by soil piping: significance and research needs, Earth-Science Reviews, Vol. 185, pp 1107-1128

Bonetti, J., Del Bianco, F., Schippa, L., Polonia, A., Stanghellini, G., Cenni, N., Draghetti, S., Marabini, F., Gasperini, L., 2022. Anatomy of Anthropically Controlled Natural Lagoons through Geophysical, Geological, and Remote Sensing Observations: The Valli Di Comacchio (NE Italy) Case Study. Remote Sensing 14, 987. https://doi.org/10.3390/rs14040987

Böhm, G., Rossi, G., Vesnaver, A., 1999. Minimum-time ray-tracing for 3-D irregular grids. Journal of seismic exploration, 8, 117-132.

Böhm, G., et al., 2014. Cat3D. Computer aided tomography for 3-D models. User Manual. OGS.

Castellarin, A., Eva, C., Giglia, G., Vai, G.B., Rabbi, E., Pini, G.A., Crestana, G., 1985. Analisi strutturale del Fronte Appennico Padano, 3ème série. ed. Istituto di geologia e paleontologia, Bologna.

Cygal, A., Stefaniuk, M., Kret, A., Kurowska, M., 2016. The application of electrical resistivity tomography (ERT), induced polarization (IP) and electromagnetic conductivity (EMC) methods for the evaluation of technical condition of flood embankment corpus. Geology, Geophysics and Environment 42, 279–279. https://doi.org/10.7494/geol.2016.42.3.279

Davis, J.L., Annan, A.P., 1989. Ground-Penetrating Radar for High-Resolution Mapping of Soil and Rock Stratigraphy. Geophysical Prospecting 37, 531–551. https://doi.org/10.1111/j.1365-2478.1989.tb02221.x

Deidda, G.P., Ranieri, G., 2005. Seismic tomography imaging of an unstable embankment. Engineering Geology 82, 32–42. https://doi.org/10.1016/j.enggeo.2005.09.017

de Oliveira, A. de O., Bonetti, J., 2021. Dynamical descriptors of physical vulnerability to sea-level rise in sheltered coastal systems: A methodological framework. Estuarine, Coastal and Shelf Science 249, 107118. https://doi.org/10.1016/j.ecss.2020.107118

Di Prinzio, M., Bittelli, M., Castellarin, A., Pisa, P.R., 2010. Application of GPR to the monitoring of river embankments. Journal of Applied Geophysics 71, 53–61. https://doi.org/10.1016/j.jappgeo.2010.04.002

Fauchard, C., Mériaux, P., 2007. Geophysical and Geotechnical Methods for Diagnosing Flood Protection Dikes. éditions Quae. https://doi.org/10.35690/978-2-7592-0035-1

Huang, J., Scudiero, E., Choo, H., Corwin, D.L., Triantafilis, J., 2016. Mapping soil moisture across an irrigated field using electromagnetic conductivity imaging. Agricultural Water Management 163, 285–294. https://doi.org/10.1016/j.agwat.2015.09.003

Inazaki, T., 2007. Integrated Geophysical Investigation For The Vulnerability Assessment Of Earthen Levee. Presented at the 20th EEGS Symposium on the Application of Geophysics to Engineering and Environmental Problems, European Association of Geoscientists & Engineers, p. cp. https://doi.org/10.3997/2214-4609-pdb.179.0101-108

Mori, G., 2009. The use of Ground Penetrating Radar and alternative geophysical techniques for assessing embankments and dykes safety (Doctoral Thesis). Alma Mater Studiorum - Università di Bologna. https://doi.org/10.6092/unibo/amsdottorato/2138

Niederleithinger, E., Weller, A., Lewis, R., 2012. Evaluation of Geophysical Techniques for Dike Inspection. Journal of Environmental and Engineering Geophysics 17, 185–195. https://doi.org/10.2113/JEEG17.4.185

Perri, M.T., Boaga, J., Bersan, S., Cassiani, G., Cola, S., Deiana, R., Simonini, P., Patti, S., 2014. River embankment characterization: The joint use of geophysical and geotechnical techniques. Journal of Applied Geophysics 110, 5–22. https://doi.org/10.1016/j.jappgeo.2014.08.012

Smith, D. G., and Jol, H. M., 1995. Ground Penetrating Radar: Antenna Frequencies and Maximum Probable Depths of Penetration in Quaternary Sediments, Journal of Applied Geophysics, Vol. 33, No. 1, pp. 93-100.

Szynkiewicz, A, 2000. GPR monitoring of earthen flood banks/levees. Proc. SPIE 4084, Eighth International Conference on Ground Penetrating Radar, (27 April 2000); https://doi.org/10.1117/12.383541

Vesnaver, A., Böhm, G., 2000. Staggered or adapted grids for seismic tomography? The Leading Edge 19, 944–950. https://doi.org/10.1190/1.1438762